

ORIGINAL ARTICLE

Open Access



# Estimation Model for Effective Thermal Conductivity of Reinforced Concrete Containing Multiple Round Rebars

Hyung Gyun Noh<sup>1</sup> , Hie Chan Kang<sup>2</sup>, Moo Hwan Kim<sup>1</sup> and Hyun Sun Park<sup>1\*</sup>

## Abstract

The objective of this research is to estimate the effective thermal conductivity model for the reinforced concrete containing round rebars. The thermal network concept and Fourier's law are used to develop a mathematical model to calculate the effective thermal conductivity ( $k_{\text{eff}}$ ) of reinforced concrete with different numbers of round rebars oriented either normal or parallel to the heat-transfer direction, and different volume fractions of steel. Model predictions generally agree well with results of numerical simulations using the finite-volume method (FVM). FVM results suggest that at fixed volume fractions of steel, the effective thermal conductivity decreases as the number of round rebars increases if the rebars are in the normal orientation but increases as the number of round rebars increases if they are in the parallel orientation. This research can be used in practical conditions to predict the effective thermal conductivity of reinforced concrete containing round rebars accurately.

**Keywords:** reinforced concrete, effective thermal conductivity, rebar orientation, volume fraction, composite materials

## 1 Background

Thermal analysis of concrete structures can be used to evaluate the insulation of buildings and to estimate the extent of concrete cracks (Kim et al. 2003). Demand for precise analysis in concrete structures is increasing, for example for analysis of heat sinks in nuclear power plants after Fukushima accident (Noh et al. 2017). Thermal conductivity of concrete is an important property for thermal analysis of concrete structures such as buildings and nuclear power plants, and in general civil engineering.

Many researchers have investigated key factors determining thermal conductivity of concrete (Kim et al. 2003; Uysal et al. 2004; Davraz et al. 2015). However, reinforced concrete that includes steel rebars is used in most concrete structures. Therefore, predicting effective thermal conductivity  $k_{\text{eff}}$  of reinforced concrete is very important

in many industries. Generally, reinforced concrete is composed of concrete and steel as composite material. Models of  $k_{\text{eff}}$  have been developed for evaluation of composite materials.

Maxwell (1904) proposed the first effective model of thermal conductivity in composite materials that included a dilute suspension of spheres of diverse size. The model is only applicable for volume fractions < 25% of spheres. The Rayleigh sphere model (Strutt 1892) assumed that spherical particles are regularly arranged in a continuous matrix. The model additionally considered thermal interaction between particles and Maxwell's model. The Rayleigh cylinder model (Pietrak and Wisniewski 2015) considered cylindrical particles placed uniformly. Noh et al. (2017) evaluated the applicability of these models to the containment wall of OPR1000, and presented a modified Rayleigh model that considers the orientations of rebar and tendons.

However, these models do not consider the number of round rebars  $N_{\text{re}}$  and their arrangement  $\theta$ ; development of such a model is the main purpose of this paper. This paper presents a mathematical model that considers one

\*Correspondence: hejsunny@postech.ac.kr

<sup>1</sup> Division of Advanced Nuclear Engineering (DANE), Pohang University of Science and Technology (POSTECH), 30, Jigok-ro 127 beon-gil, Nam-gu, Pohang-si, Gyeongsangbuk-do 37673, Republic of Korea  
Full list of author information is available at the end of the article  
Journal information: ISSN 1976-0485 / eISSN 2234-1315

round rebar or multiple round rebars; the model uses the thermal network concept and Fourier’s law. The model considers  $N_{re}$  and their orientations (normal to  $(\theta_{\perp})$  or parallel to  $(\theta_{\parallel})$  the heat-flow direction) at the same volume fraction  $\Phi_s$  of steel. This model can predict  $k_{eff}$  at various geometries in practical use.

Numerical simulations were performed to validate the mathematical model with  $\sim 1\% \leq \Phi_s \leq 14\%$  of rebars based on KS R 3504. Numerical simulations also consider  $N_{re}$  and  $\theta$ . Results suggest that at a given  $\Phi_s$ ,  $k_{eff}$  decreases as  $N_{re}$  increases if the rebars are in the  $\theta_{\perp}$  orientation, but increases as  $N_{re}$  increases if they are in the  $\theta_{\parallel}$  orientation. The proposed model could increase the accuracy of thermal analysis in structures that use reinforced concrete.

## 2 Modeling Method

A thermal resistance network is a useful way to model  $k_{eff}$  theoretically in composite materials (Agrawal and Satapathy 2015). The method assumes that the heat transfer is adiabatic in any plane parallel to the heat-flow direction. Two models are developed; one considers reinforced concrete containing one round rebar (Fig. 1) and one considers multiple round rebars (Fig. 2).  $k_{eff}$  model at the reinforced concrete can be derived by solving complex thermal network and using Fourier’s law (Figs. 3, 4). The equations are developed as follows.

### 2.1 Reinforced Concrete Containing One Round Rebar

The concrete is modelled as a cube with side length  $L$ . The block can be divided into concrete and steel components (Fig. 3, left). The corresponding thermal network (Fig. 3, right) to model reinforced concrete with  $N_{re}=1$  is composed of five thermal resistances. The

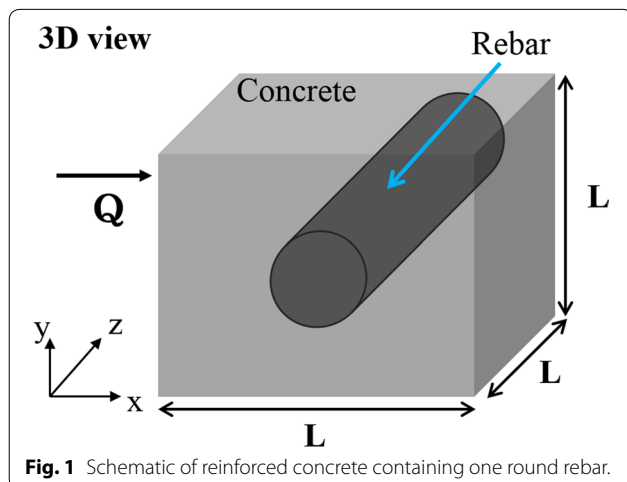
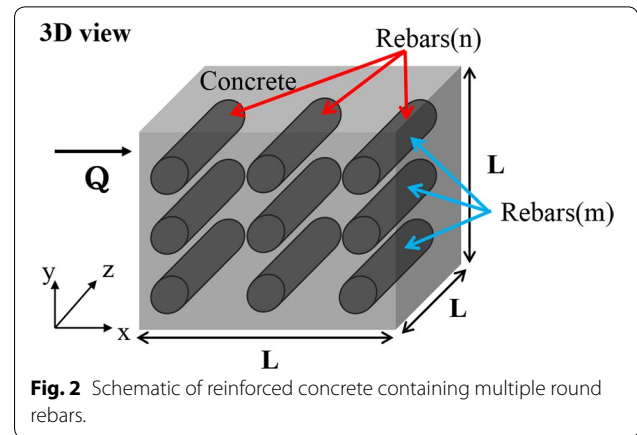


Fig. 1 Schematic of reinforced concrete containing one round rebar.



round rebar is oriented along the  $z$  axis in the concrete, and heat is applied along the  $x$  axis. The  $k_{eff}$  model can be derived by developing the following equations as function of  $\Phi_s$ , and the thermal conductivities of concrete and of steel.

$$\frac{1}{R_{total}} = \frac{1}{R_1} + \frac{1}{R_2} + \frac{1}{R_3} \tag{1}$$

$$\frac{1}{R_1} + \frac{1}{R_3} = \frac{k_c}{L} (A_1 + A_3) \left( \because k_1 = k_3 = k_c, R = \frac{L}{kA} \right). \tag{2}$$

To calculate  $R_2$ , formulas are developed in sequence

$$R_2 = R_{2,1} + R_{2,2} + R_{2,3}. \tag{3}$$

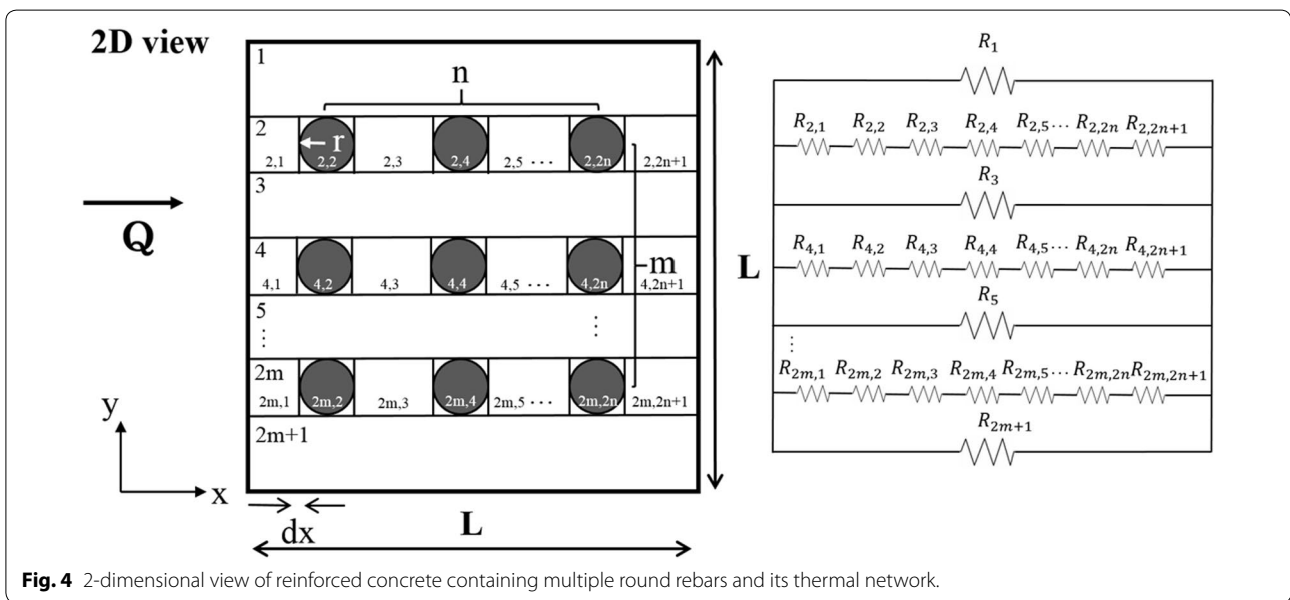
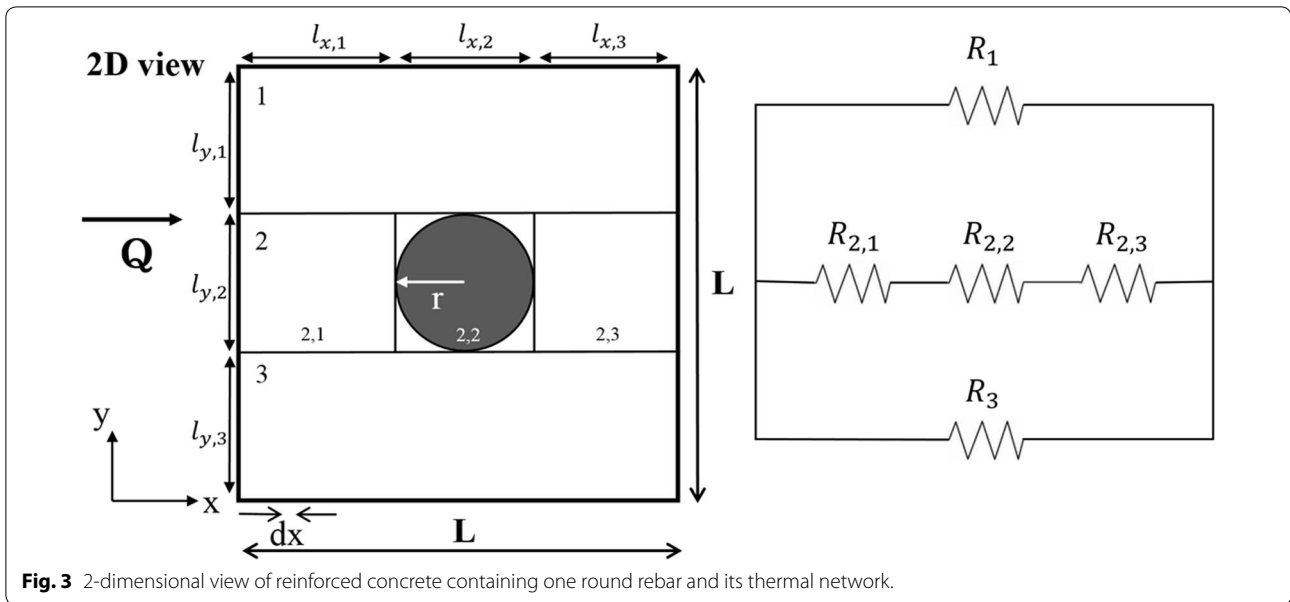
$$R_{2,1} + R_{2,3} = \frac{L - 2r}{k_c A_2} \quad (\because l_{x,1} + l_{x,3} = L - 2r). \tag{4}$$

$$Q_{total} = Q_s + Q_c \text{ at } R_{2,2}. \tag{5}$$

$$k_{2,2} = \frac{Q_s + Q_c}{\frac{dT}{dx} \cdot A_2} = \frac{k_s A_s}{A_2} + \frac{k_c A_c}{A_2} \quad \left( \because Q = kA \frac{dT}{dx} \right). \tag{6}$$

Two-dimensional integration over  $2r$  is performed to obtain the value of in Eq. (6) because  $A_s$  and  $A_c$  are expressed as functions of  $x$ . For convenience of calculation, the coordinate at the center of the round rebar is set to  $(0,0)$ .

$$A_s(x) = 2yL = 2(r^2 - x^2)^{\frac{1}{2}}L \quad (\because x^2 + y^2 = r^2), \tag{7}$$



$$A_c(x) = 2rL - 2yL = 2rL - 2(r^2 - x^2)^{\frac{1}{2}}L. \tag{8}$$

$A_s(x)$  and  $A_c(x)$  are inserted into Eq. (6), then  $k_{2,2}$  can be derived as

$$\begin{aligned} k_{2,2} &= \frac{1}{2rA_2} \int_{-r}^r (k_s A_s + k_c A_c) dx \\ &= \frac{1}{2rA_2} \int_{-r}^r (2k_s(r^2 - x^2)^{\frac{1}{2}}L \\ &\quad + k_c(2rL - 2(r^2 - x^2)^{\frac{1}{2}}L)) dx \end{aligned} \tag{9}$$

To enable simple solution of the formula,  $r \sin(u)$  is substituted for  $x$

$$\begin{aligned} k_{2,2} &= \frac{k_s \cdot 2L}{2rA_2} \left[ \frac{x\sqrt{r^2 - x^2}}{2} - \frac{r^2}{2} \arcsin \frac{x}{r} \right]_{-r}^r \\ &\quad + \frac{k_c}{2rA_2} \left[ 2rLx - 2L \left( \frac{x\sqrt{r^2 - x^2}}{2} - \frac{r^2}{2} \arcsin \frac{x}{r} \right) \right]_{-r}^r \\ &= \frac{1}{2rA_2} k_s (\pi r^2 L) + \frac{1}{2rA_2} k_c (4r^2 L - \pi r^2 L) \end{aligned} \tag{10}$$

$$R_{2,2} = \frac{4r^2}{k_s(\pi r^2 L) + k_c(4r^2 L - \pi r^2 L)} \quad (11)$$

Thus,  $R_2$  can be expressed as

$$R_2 = \frac{L - 2r}{k_c A_2} + \frac{4r^2}{k_s(\pi r^2 L) + k_c(4r^2 L - \pi r^2 L)} \quad (12)$$

Moreover, total thermal network can be expressed as

$$R_{total} = \frac{1}{\frac{1}{R_1} + \frac{1}{R_2} + \frac{1}{R_3}}, \quad (13)$$

$$k_{eff} = \frac{L}{R_{total} \cdot A} \quad (14)$$

Therefore,  $k_{eff}$  can be derived as (15). Detailed calculation is omitted.

$$\begin{aligned} \therefore k_{eff} = k_c & \left[ 1 - \left( \frac{4\phi_s}{\pi} \right)^{1/2} \right] \\ & + \frac{1}{\frac{1}{k_c} \left[ \left( \frac{\pi}{4\phi_s} \right)^{1/2} - 1 \right] + \frac{4}{\pi(k_s - k_c) + 4k_c}}, \quad (15) \\ & \left( \because \phi_s = \frac{\pi r^2}{L^2} \right). \end{aligned}$$

Due to mathematical conditions,  $2r$  must be  $< L$  ( $\phi_s < 0.7854$ ), so  $\phi_s$  should not exceed 0.7854.

### 2.2 Reinforced Concrete Containing Multiple Round Rebars

This model also considers a concrete cube of side  $L$ . All round rebars are oriented along the  $z$  axis (Fig. 2). In this model,  $m$  rows of  $n$  round rebars are embedded in reinforced concrete.  $k_{eff}$  models consider rebars in the  $\theta_{\perp}$  and  $\theta_{\parallel}$  orientations. The  $k_{eff}$  model of reinforced

concrete containing multiple round rebars can be acquired by solving complex thermal network (Fig. 4). The thermal network including many round rebars can be generally expressed in two parts: concrete layer that is modelled by using the thermal resistance of concrete; and a mixed layer composed of alternating thermal resistances of concrete and steel. The two layers are stacked alternately beginning and ending with concrete layers (Fig. 4). The theoretical model of  $k_{eff}$  is derived as follows.

Total thermal network can be represented as the sum of the two major parts:

$$\frac{1}{R_{total}} = \frac{1}{R_1} + \frac{1}{R_2} + \frac{1}{R_3} + \dots + \frac{1}{R_{2m+1}}. \quad (16)$$

The concrete zone is described as

$$\begin{aligned} S_o &= \frac{1}{R_1} + \frac{1}{R_3} + \dots + \frac{1}{R_{2m+1}} \\ &= \frac{k_c}{L} (A_1 + A_3 + \dots + A_{2m+1}), \quad (17) \end{aligned}$$

and mixed zone is also given as follow:

$$S_e = \frac{1}{R_2} + \frac{1}{R_4} + \dots + \frac{1}{R_{2m}} = \frac{m}{R_2} \quad (18)$$

To obtain  $R_2$ , the formula is derived sequentially:

$$R_2 = R_{2,1} + R_{2,2} + R_{2,3} + \dots + R_{2,2n+1}, \quad (19)$$

$$R_{2,o} = R_{2,1} + R_{2,3} + \dots + R_{2,2n+1} = \frac{L - 2rn}{k_c A_2} \quad (20)$$

$$R_{2,e} = R_{2,2} + R_{2,4} + \dots + R_{2,2n} = nR_{2,2} \quad (21)$$

Integration is conducted over  $2r$  to obtain  $R_{2,2}$  on  $k_{2,2}$ ; the process is the same as in Sect. 2.1, so details are omitted. Thus,  $R_2$  can be expressed as

$$R_2 = \frac{L - 2rn}{k_c A_2} + \frac{4nr^2}{k_s(\pi r^2 L) + k_c(4r^2 L - \pi r^2 L)} \quad (22)$$

**Table 1 Thermal properties of reinforced concrete.**

Material	Thermal properties			Remarks
	Density (kg/m <sup>3</sup> )	Heat capacity (J/(kg K))	Thermal conductivity (W/(m K))	
Concrete (1:2:4)	2200	654	1.6	Korean Ministry of Land, Infrastructure and Transport (KMOLIT) (2015)
Steel	7900	503	53	

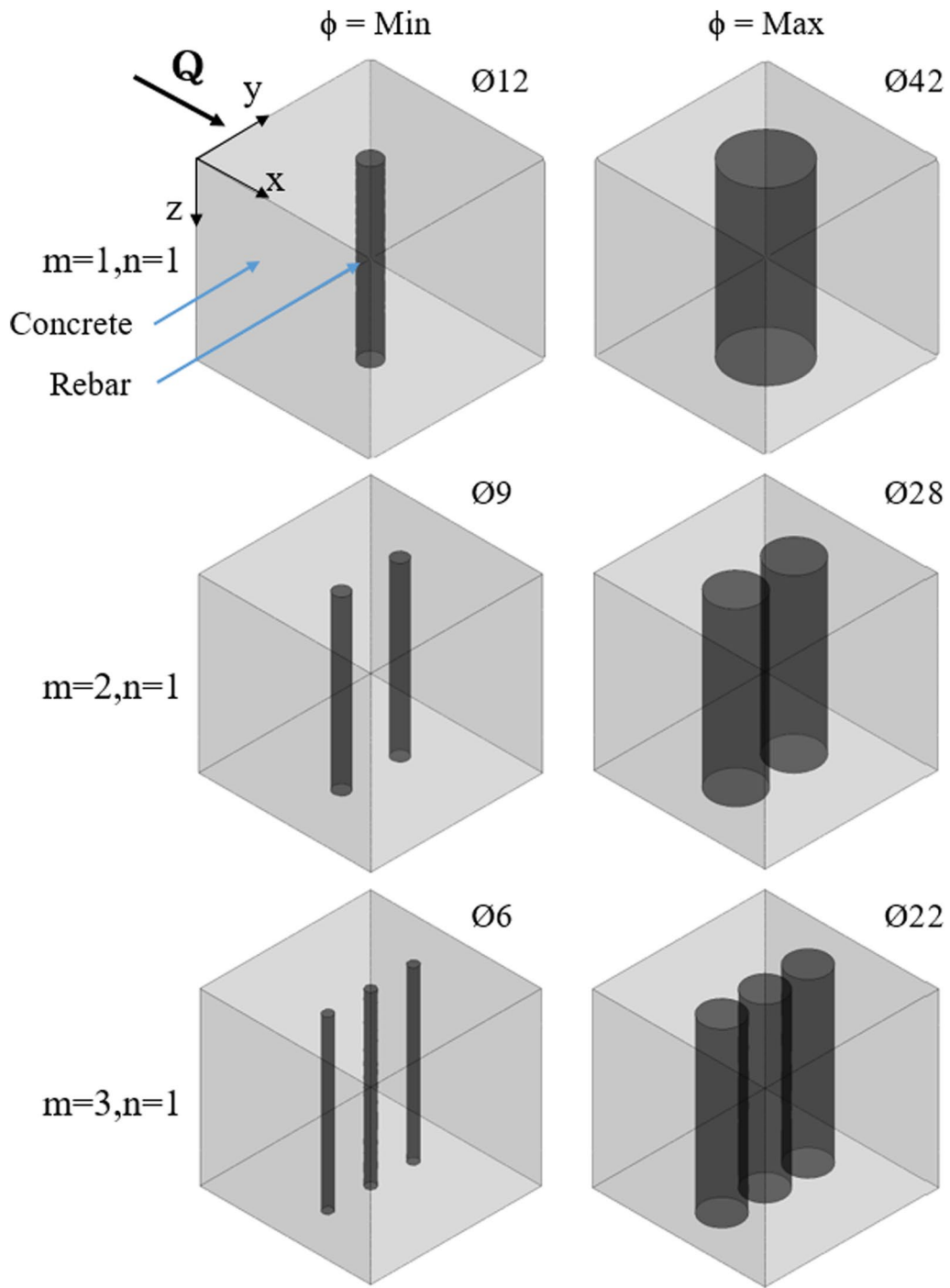


**Fig. 5** Numerical domain in reinforced concrete as volume fraction and the number of rebars.

Therefore,  $k_{eff}$  can be expressed by deriving equation of  $R_{total}$  (23). Calculation details are omitted.

$$\begin{aligned} \therefore k_{eff} = & k_c \left[ 1 - \left( \frac{4m\phi_s}{n\pi} \right)^{1/2} \right] \\ & + \frac{m}{\frac{1}{k_c} \left[ \left( \frac{mn\pi}{4\phi_s} \right)^{1/2} - n \right] + \frac{4n}{\pi(k_s - k_c) + 4k_c}} \\ & \left( \because \phi_s = \frac{m \cdot n \cdot \pi r^2}{L^2} \right). \end{aligned} \quad (23)$$

Because  $2mr$  and  $2nr$  must both be  $<L$ ,  $\Phi_S$  must simultaneously be  $<n\pi/(4m)$  and  $<m\pi/(4n)$ .

### 3 Numerical Simulations

The numerical simulations to analyze the  $k_{eff}$  of reinforced concrete as  $\Phi_S$  and  $N_{re}$  were performed using ANSYS CFX16.2 in the steady-state condition. The Finite Volume Method (FVM) adopted by ANSYS CFX16.2 is used for numerical simulations because it conserves mass, momentum, and energy better than the Finite Difference Method (FDM) does. Thermal properties (Table 1) for the numerical simulations are based on the Korean design standard of buildings (Korean Ministry of Land, Infrastructure and Transport (KMOLIT) 2015).

The numerical domain is a cube with side length 0.1 m. Thirty test cases are conducted with various  $\Phi_S$  and  $N_{re}$ .

**Table 2 Test cases for the numerical simulations of  $k_{eff}$  in reinforced concrete.**

Number of round rebars	Diameter of round rebar (mm) (KS R 3504)	Volume fraction (%)	$m \times n$
1	12	1.13	1 × 1
	16	2.01	
	22	3.80	
	28	6.16	
	36	10.18	
	42	13.85	
2	9	1.27	1 × 2, 2 × 1
	13	2.65	
	16	4.02	
	22	7.60	
	25	9.82	
	28	12.31	
	3	6	
9	1.91		
13	3.98		
16	6.03		
19	8.50		
22	11.40		

The rebars have diameters of 6–42 mm, following KS R 3504 for practical and actual uses of reinforced concrete (Fig. 5), with  $\sim 1\% \leq \Phi_S \leq \sim 14\%$  (Table 2).

Conditions of the simulations are as follows. The contact thermal resistance between concrete and steel is neglected. For the boundary conditions, constant heat flux is applied to the inside surface of the concrete wall and constant convective heat transfer coefficient and room temperature are adopted at the outside air of the concrete surface (Fig. 6). Adiabatic conditions in the heat transfer direction are assumed at the four surfaces.

Convergence is assumed when residuals are  $<10^{-10}$  and energy balance was  $>99.9\%$ . Tetrahedron grid is used as mesh type and the number of grids is about 0.92 million. For verification, numerical simulation was conducted using concrete with no rebar. To confirm that the boundary conditions did not effect  $k_{eff}$ , additional numerical analysis was conducted that considered heat flux inside the concrete, and heat transfer coefficient and temperature of the outside air.

### 4 Results and Discussion

$k_{eff}$  of reinforced concrete containing multiple round rebars was numerically determined versus  $\Phi_S$ , and  $N_{re}$  and  $\theta$ . The average temperature gradually decreases as  $\Phi_S$  increases at the left side of concrete wall (Figs. 7, 8); this trend means that  $k_{eff}$  of reinforced concrete increases as  $\Phi_S$  increases.

As the number  $m$  of rows of rebars increases, temperature field becomes uniform. Increase in  $m$  affects the reduction of  $k_{eff}$  at the same  $\Phi_S$  (Fig. 7). On the contrary, as the number  $n$  of rebars in a row increases, the temperature field becomes distorted; increase in  $n$  has a significant effect on the increase in  $k_{eff}$  at the same  $\Phi_S$  (Fig. 8).

To evaluate how  $\Phi_S$  and  $N_{re}$  affected the  $k_{eff}$  of reinforced concrete, the results of FVM were compared with the mathematical model. Considering  $m$ , the model results for reinforced concrete with rebars in the  $\theta_{\perp}$

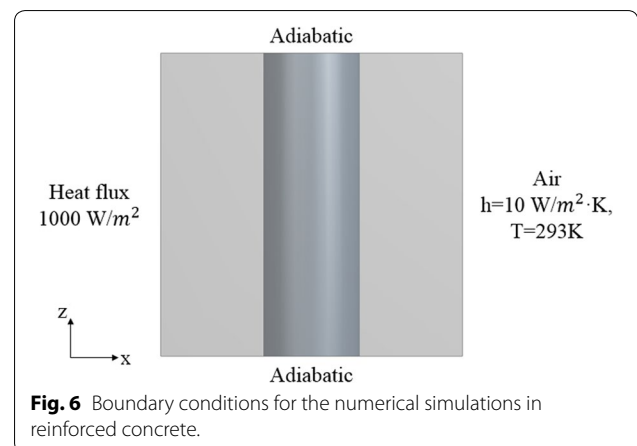


**Fig. 6** Boundary conditions for the numerical simulations in reinforced concrete.

orientation matches the results of FVM (Fig. 9) with a standard deviation of 0.41–0.43% and a maximum error of ~1.5%. The large discrepancy is shown between sphere models and the numerical simulation due to difference of shape. Rayleigh cylinder model can't estimate reduction of  $k_{eff}$  as increasing  $m$ .

Considering  $n$ , the model also well predict the results of FVM when the rebars in the  $\theta_{\parallel}$  orientation (Fig. 10), with a standard deviation of 0.31–1.05% and maximum error of ~2.8%. The highest discrepancy between model value and results of FVM occurs with  $n=3$  at the largest  $\Phi_S$ . This tendency may be due to temperature distortion at

both concrete walls (Fig. 8). Sphere models and cylinder model are hard to explain this tendency of  $k_{eff}$  depending on  $n$  due to different shape and assumption of regular arrangement.

$k_{eff}$  of reinforced concrete containing rebars is strongly affected by  $\Phi_S$  at the same  $N_{re}$ .  $k_{eff}$  decreases as  $N_{re}$  increases if the rebars are in the  $\theta_{\perp}$  orientation, but increases as  $N_{re}$  increases if they are in the  $\theta_{\parallel}$  orientation. For reinforced concrete with  $N_{re}=1$ , a correlation from FVM is expressed as a function of  $\Phi_S$  as

$$k_{eff} = 3.457^2 + 2.925 + 1.598, \quad (0 \ll 0.15) \quad (24)$$

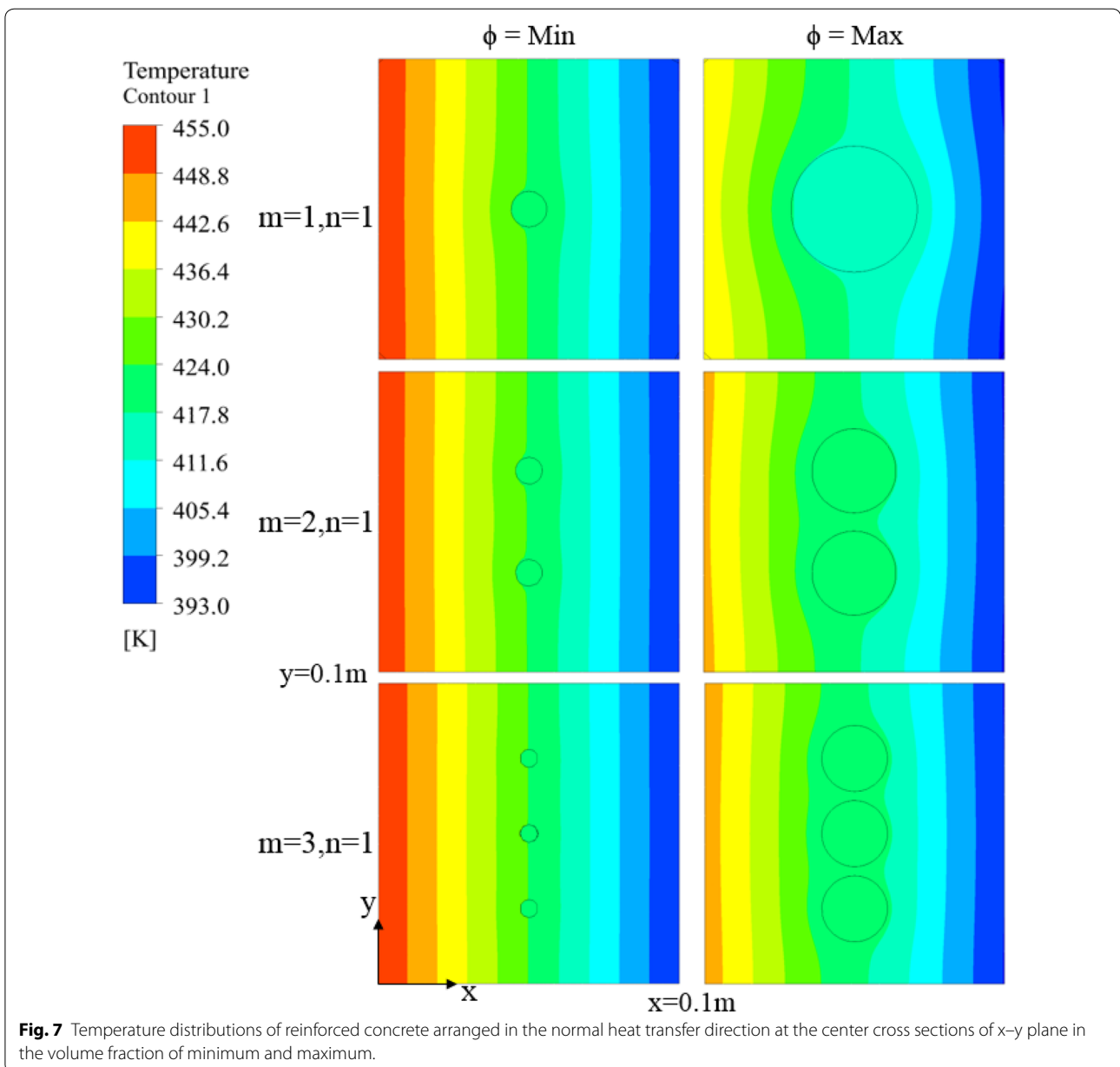


**Fig. 7** Temperature distributions of reinforced concrete arranged in the normal heat transfer direction at the center cross sections of x-y plane in the volume fraction of minimum and maximum.

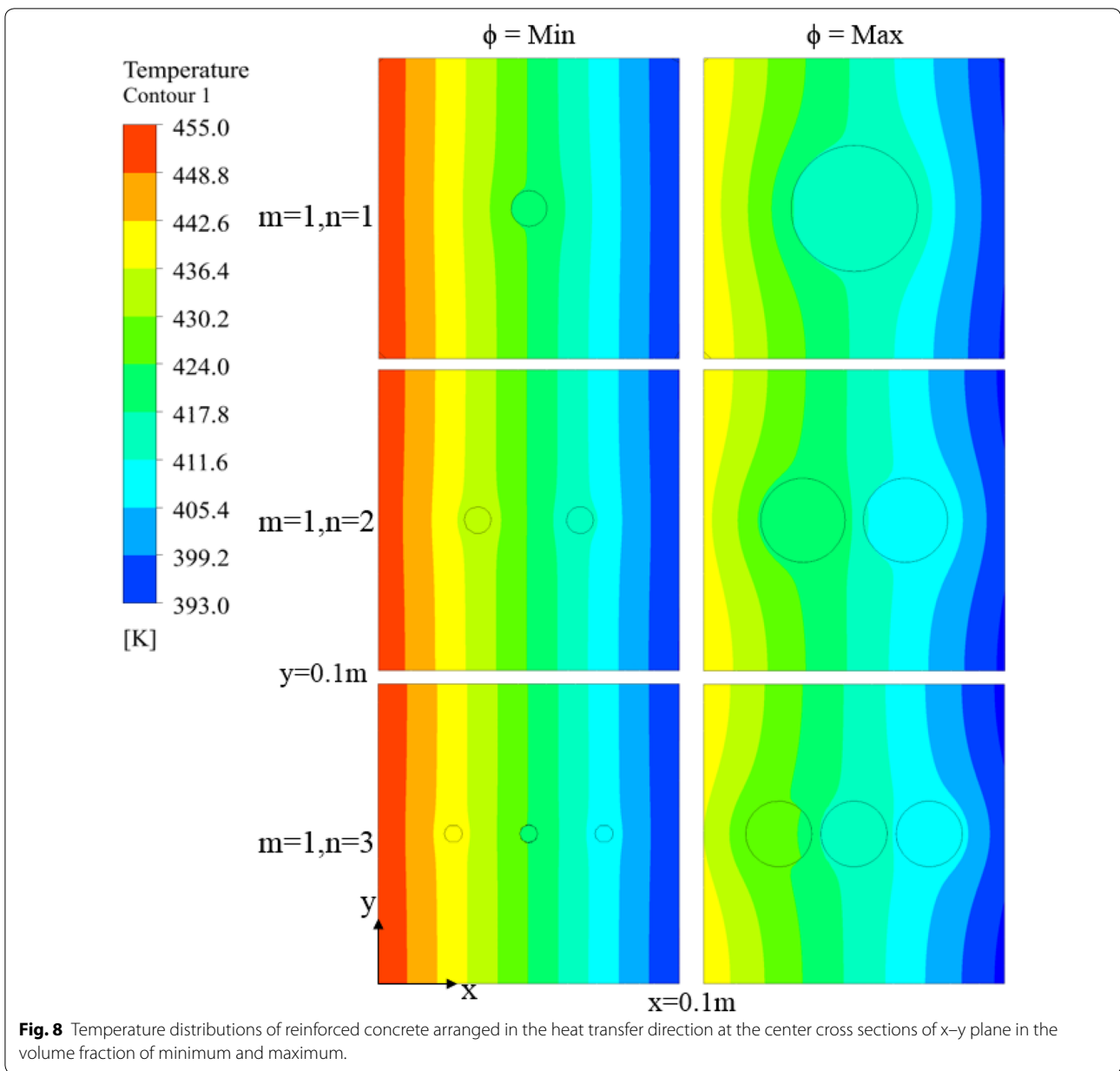


**Fig. 8** Temperature distributions of reinforced concrete arranged in the heat transfer direction at the center cross sections of x-y plane in the volume fraction of minimum and maximum.

Experimental data, FVM results, and  $k_{eff}$  models predictions are represented over  $\Phi_s$  (Fig. 11). Thermal conductivity of concrete varies with conditions such as density, w/c ratio and its types; therefore, non-dimensional  $k_{eff}$  is used for quantitative comparison at identical conditions. As supplementary information, we consider the results of Zhao et al. who manufactured reinforced concrete with rebars in the  $\theta_{\perp}$  orientation (Zhao et al. 2013); the rebars are inserted horizontally at the center of the concrete specimen;  $\Phi_s$  is 1.7 and 2.7%. In Zhao's experiment,  $k_{eff}$  is 1.4313 W/(m K) in the bare concrete, 1.5145 W/(m K) in the reinforced concrete with

$\Phi_s = 1.7\%$ , and 1.5524 W/(m K) in the reinforced concrete with  $\Phi_s = 2.7\%$ . The mathematical model predicts Zhao's experimental data well, with error of 3.38% in the reinforced concrete with  $\Phi_s = 1.7$  and 4.53% in the reinforced concrete with  $\Phi_s = 2.7\%$ . Overall, the mathematical model matches the results of FVM well, with average standard deviation of 0.52%.

### 5 Conclusion

This paper presents a model based on the thermal network concept and Fourier's law, a model to predict the effective thermal conductivity ( $k_{eff}$ ) of reinforced concrete

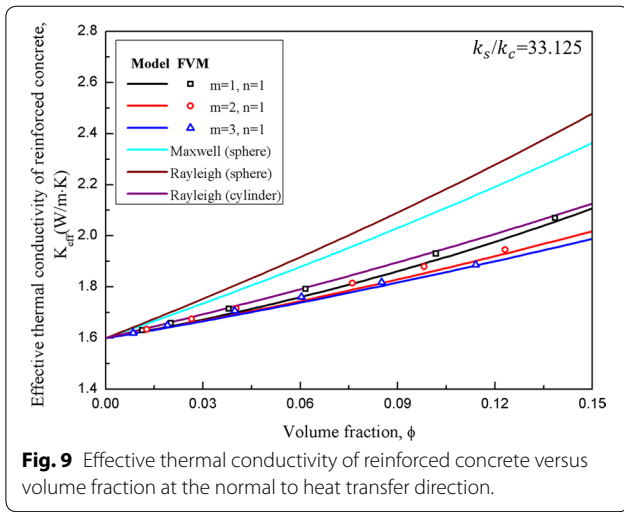


**Fig. 9** Effective thermal conductivity of reinforced concrete versus volume fraction at the normal to heat transfer direction.

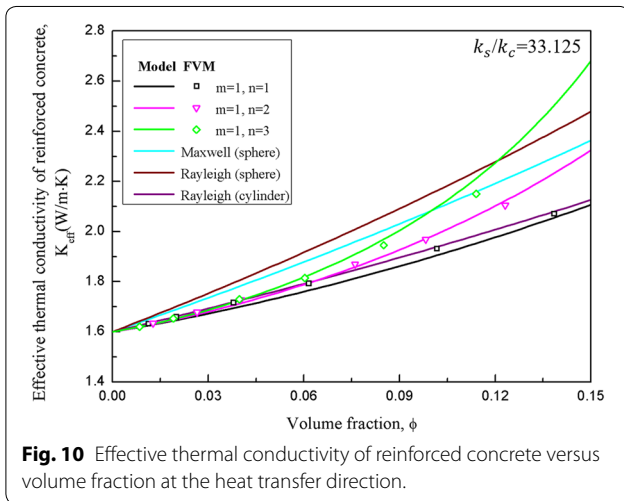


**Fig. 10** Effective thermal conductivity of reinforced concrete versus volume fraction at the heat transfer direction.

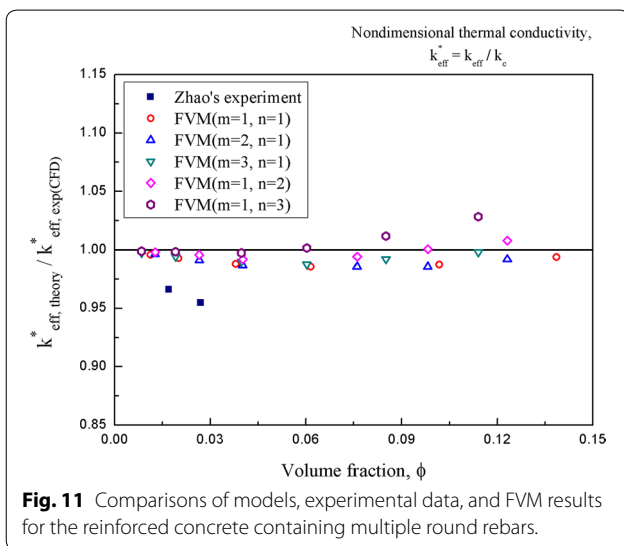


**Fig. 11** Comparisons of models, experimental data, and FVM results for the reinforced concrete containing multiple round rebars.

containing round rebars. To validate the mathematical models for the effective thermal of reinforced concrete containing round rebars oriented normal ( $\theta_{\perp}$ ) or parallel ( $\theta_{\parallel}$ ) to the heat-flow direction was investigated numerically using ANSYS CFX16.2. Mathematical models were compared with FVM results at various volume fraction of steel, number of rebars and orientations of rebars. At the same number of rebars, the effective thermal conductivity of reinforced concrete is affected by volume fraction of steel. Furthermore, at the same volume fraction of steel, the effective thermal conductivity decreases as the number of rebars increases if the rebars are in the  $\theta_{\perp}$  orientation, but increases as the number of rebars increases if they are in the  $\theta_{\parallel}$  orientation. The mathematical model generally matches the results of FVM well. The average standard deviation between models and FVM results is 0.52%. The small magnitude of this disagreement indicates that these mathematical models can be used to estimate  $k_{eff}$  of reinforced concrete containing multiple round rebars at volume fraction of steel less than 15%.

This research has developed a reliable mathematical model to predict the effective thermal conductivity of reinforced concrete containing round rebars. However, to increase the adhesion between rebar and concrete, many industries generally use deformed rebars that have ribs and nodes. Nevertheless, ribs and nodes increase the volume fraction of steel contribution of the bar only slightly. Therefore, this model could be also applicable to reinforced concrete that uses rebars that have ribs and nodes, because their effect on volume fraction of steel is probably negligible.

**List of symbols**

$A_c$ : area of concrete in mixed part ( $m^2$ );  $A_s$ : area of steel in mixed part ( $m^2$ );  $A_i$ : area of  $i$ th section ( $m^2$ );  $k_{eff}$ : effective thermal conductivity in reinforced concrete ( $W/(m K)$ );  $k_c$ : concrete thermal conductivity ( $W/(m K)$ );  $k_s$ : steel thermal conductivity ( $W/(m K)$ );  $l_{ij}$ :  $j$ th length of  $i$  direction ( $m$ );  $L$ : one side length of concrete wall ( $m$ );  $m$ : the number of round rebars at normal to heat transfer direction;  $n$ : the number of round rebars at parallel to heat transfer direction;  $N_{re}$ : number of rebars in the unit cell;  $R_{total}$ : total thermal resistance ( $K/W$ );  $R_i$ :  $i$ th thermal resistance ( $K/W$ );  $Q_{total}$ : total heat quantity ( $W$ );  $Q_c$ : heat quantity to concrete ( $W$ );  $Q_s$ : heat quantity to steel ( $W$ );  $S_o$ : sum of one over odd number thermal resistance ( $W/K$ );  $S_e$ : sum of one over even number thermal resistance ( $W/K$ );  $r$ : radius of round rebar ( $m$ );  $\phi_s$ : volume fraction of steel;  $\theta$ : orientation of rebar;  $\theta_{\perp}$ : orientation of rebar normal to heat-transfer direction;  $\theta_{\parallel}$ : orientation of rebar parallel to heat-transfer direction.

**Authors' contributions**

HGN carried out the effective thermal conductivity studies of concrete, participated in the sequence alignment and drafted the manuscript. HCK participated in discussing modeling part of this research, specifically. MHK discussed about the overall research such as introduction, result and conclusion parts. HSP conducted optimization of this study. Moreover, He mainly participated in result graphs. All authors read and approved the final manuscript.

**Author details**

<sup>1</sup> Division of Advanced Nuclear Engineering (DANE), Pohang University of Science and Technology (POSTECH), 30, Jigok-ro 127 beon-gil, Nam-gu, Pohang-si, Gyeongsangbuk-do 37673, Republic of Korea. <sup>2</sup> Mechanical

Engineering Division, Kunsan National University (KNU), 558, Daehak-ro, Gunsan-si, Jeollabuk-do 54150, Republic of Korea.

#### Acknowledgements

This work was supported by the Nuclear Safety Research Program through the Korea Foundation of Nuclear Safety (KOFONS), granted financial resource from the Nuclear Safety and Security Commission (NSSC), Republic of Korea (No. 1305008).

#### Competing interests

The authors declare that they have no competing interests.

#### Publisher's Note

Springer Nature remains neutral with regard to jurisdictional claims in published maps and institutional affiliations.

Received: 3 August 2017 Accepted: 26 June 2018

Published online: 05 October 2018

#### References

- Agrawal, A., & Satapathy, A. (2015). Mathematical model for evaluating effective thermal conductivity of polymer composites with hybrid fillers. *International Journal of Thermal Sciences*, *89*, 203–209.
- Davraz, M., Koru, M., & Akdag, A. E. (2015). The effect of physical properties on thermal conductivity of lightweight aggregate. *Procedia Earth and Planetary Science*, *15*, 85–92.
- Kim, K. H., Jeon, S. E., Kim, J. K., & Yang, S. (2003). An experimental study on thermal conductivity of concrete. *Cement and Concrete Research*, *33*, 363–371.
- Korean Ministry of Land, Infrastructure and Transport (KMOLIT), Energy conserving design criteria of building. Section No. 2015–1108. Article 6 mandatory of architectural department, 2015.
- Maxwell, J. C. (1904). *A treatise on electricity and magnetism* (3rd ed., Vol. I). Oxford: Oxford University Press.
- Noh, H. G., Lee, J. H., Kang, H. C., & Park, H. S. (2017). Effective thermal conductivity and diffusivity of containment wall as heat sink for nuclear power plant OPR1000. *Nuclear Engineering and Technology*, *49*, 459–465.
- Pietrak, K., & Wisniewski, T. S. (2015). A review of models for effective thermal conductivity of composite materials. *Journal of Power Technologies*, *95*, 14–24.
- Strutt, J. (Lord Rayleigh). (1892). On the influence of obstacles arranged in rectangular order upon the properties of a medium. *Philosophical Magazine*.
- Uysal, H., Demirboga, R., Sahin, R., & Gul, R. (2004). The effects of different cement dosages, slumps, and pumice aggregate ratios on the thermal conductivity and density of concrete. *Cement and Concrete Research*, *34*, 845–848.
- Zhao, S., Yang, S., Feng, X., & Lu, M. (2013). Study on thermal conductivity of reinforced concrete plate. *Applied Mechanics and Materials*, *438–439*, 321–328.

Submit your manuscript to a SpringerOpen<sup>®</sup> journal and benefit from:

- Convenient online submission
- Rigorous peer review
- Open access: articles freely available online
- High visibility within the field
- Retaining the copyright to your article

Submit your next manuscript at ► [springeropen.com](http://springeropen.com)